

Measurement of the deuteron coalescence probability in jets with ALICE

Marika Rasà^{a,b,*} on behalf of the ALICE Collaboration

^a*Department of Physics and Astronomy "E. Majorana", University of Catania*

Via S. Sofia 64, Catania, Italy

^b*INFN, Section of Catania,*

Via S. Sofia 64, Catania, Italy

E-mail: marika.rasa@cern.ch

The microscopic production mechanism of light (anti)nuclei in high-energy hadronic collisions is still mysterious and is a highly debated topic in the scientific community. Two different phenomenological models are typically used to describe the experimental data: the statistical hadronization model and baryon coalescence. In the former, light nuclei are emitted from a source in local thermal and hadrochemical equilibrium. Their yields are calculated using the QCD partition function by imposing the conservation of quantum numbers inside the so-called correlation volume. In the coalescence approach, light nuclei can be formed if the phase-space configuration of nucleons at kinetic freezeout is compatible with the Wigner density of the bound state. A straightforward prediction of the coalescence model is an enhanced coalescence probability of nuclei inside jets compared to that in the underlying event, measured in small collision systems: this enhancement is due to the reduced distance in phase-space between nucleons in jets compared to hadrons outside of jets.

In this contribution, the p_T -differential production yields and coalescence parameter of (anti)deuterons inside jets and in the underlying event measured by ALICE in small collision systems are presented. These results are compared to expectations from coalescence and a reaction-based model. In the latter approach, implemented in the PYTHIA 8.3 event generator, deuterons are generated using ordinary nuclear reactions.

HardProbes2023

26-31 March 2023

Aschaffenburg, Germany

*Speaker

1. Introduction

The production of light (anti)nuclei has been extensively studied in different experiments, ranging from low collisions energies at the AGS [1]-[2] to higher energies at RHIC [3]-[5] and LHC [6]-[13]. Despite this, the production mechanism of light (anti)nuclei is still unclear and it is a highly debated topic in the scientific community. Two phenomenological models are commonly used to describe this process: the Standard Hadronization Model (SHM) [14] and the coalescence model [15]. In the SHM the hadrons are emitted by a thermally and chemically equilibrated source at the kinetic freeze-out, with the abundances of each species fixed at the freeze out. This model provides good description of the particles abundance in central heavy-ion collisions [16], with a common chemical freeze out temperature of about 156 MeV, but fails to reproduce the results on hypertriton production in small systems [13]. Moreover, the SHM is a macroscopic model, and the description of the hadron formation is not addressed in detail.

In the coalescence model, if the nucleons are close in the phase space and their spin states are compatible with that of the bound state they can bind and form a nucleus. More advanced implementations of the coalescence model are available using the Wigner formalism, where both the source size and the dependence of the wave function of the bound state are taken into account. Different parametrizations of the wave function are available: the best results for the deuteron coalescence probability are obtained with the Argonne ν_{18} wave function, a phenomenological potential constrained to proton-neutron scattering measurements [17]. The coalescence probability is linked to an experimental observable, the coalescence parameter B_A , defined as

$$B_A = \left(\frac{1}{2\pi p_T^A} \frac{d^2 N_A}{dy dp_T^A} \right) \bigg/ \left(\frac{1}{2\pi p_T^p} \frac{d^2 N_p}{dy dp_T^p} \right)^A \quad (1)$$

where A is the mass number of the formed nucleus, and the invariant spectra of the (anti)protons is evaluated at the transverse momentum of the (anti)nucleus divided by its mass number. In such model, the proton and neutron production spectra are assumed the same, since they belong to the same isospin doublet.

A straightforward prediction of the coalescence model is the enhancement of the coalescence parameter in jets with respect to the same quantity in the underlying event, due to the reduced distance in phase-space between nucleons in jets compared to hadrons outside of jets. In this case to reconstruct the jet, instead of using the jet finder algorithm, a simpler approach is used: the particle in the event with the highest p_T and higher than a threshold fixed to 5 GeV/ c is used as proxy of the jet axis, and an azimuthal angle $\phi = 0$ is assigned to it. Then, all the other particles are classified in three azimuthal regions accordingly to the $\Delta\phi$ with respect to the leading particle: the Toward region ($|\Delta\phi| < 60^\circ$) that contains both the jet contribution and the underlying event, the Away region ($|\Delta\phi| > 120^\circ$) that is characterized by the recoil jet and the underlying event, and the Transverse region ($60^\circ < |\Delta\phi| < 120^\circ$) dominated by the underlying event. In order to extract the spectra in the jet, a subtraction between the Toward and the Transverse region is performed.

In this paper, the (anti)deuteron production and the corresponding coalescence parameter in jet and in underlying event in pp collisions at $\sqrt{s} = 13$ TeV [18] and p-Pb collisions at $\sqrt{s_{NN}} = 5.02$ TeV are discussed. To identify the produced particles, the Time Projection Chamber (TPC) and Time Of Flight (TOF) detectors of the ALICE experiment, discussed in detail in Ref. [19], are

used. Additional considerations are made for the pp collisions, discussing the comparison of the experimental results with the prediction of the models.

2. (Anti)deuteron production and coalescence parameter

The (anti)deuteron production in jet and underlying event is studied in pp collisions at $\sqrt{s} = 13$ TeV and p–Pb collisions at $\sqrt{s_{NN}} = 5.02$. To evaluate the coalescence parameter, the transverse momentum spectra of (anti)deuteron is needed. These spectra are shown in Fig. 1, considering the three azimuthal regions and the in-jet region, for pp (upper row) and p–Pb (lower row) collisions.

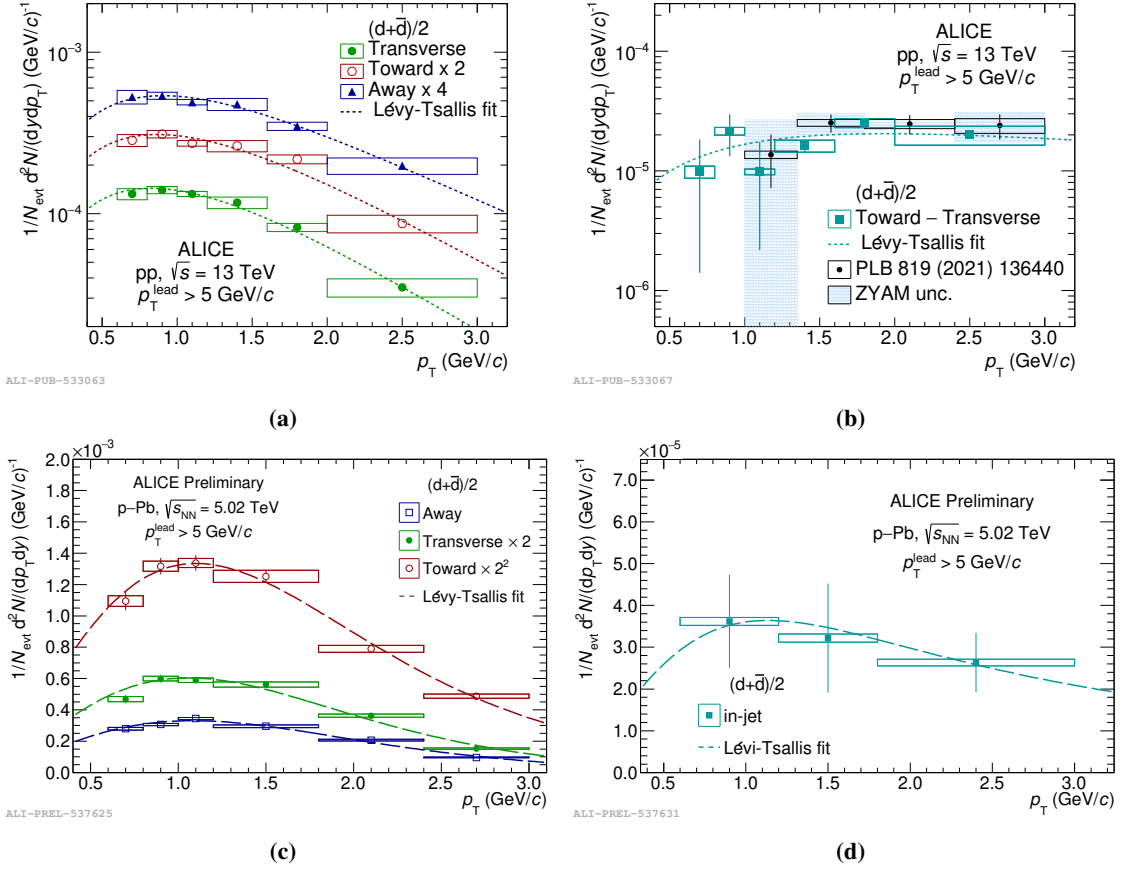


Figure 1: Transverse momentum spectra of (anti)deuteron in the three azimuthal regions and in jet for pp collisions at $\sqrt{s} = 13$ TeV (panels (a) and (b) respectively) [18] and for p–Pb collisions at $\sqrt{s_{NN}} = 5.02$ TeV (panels (c) and (d) respectively). Vertical bars represent the statistical uncertainties while boxes represent the systematic uncertainties, and the dashed line is the Lévy-Tsallis fit. In both systems, the Toward region is in red, the Transverse region in green, the Away region in blue and the in-jet contribution is cyan.

A similar study is also performed to obtain the (anti)proton spectra, that is evaluated in the p_T region between 0.3 and 1.5 GeV/c , since the coalescence parameter B_2 is evaluated as a function of the transverse momentum divided by the mass number of the nucleus, in this case the deuteron. Then the coalescence parameter is calculated using the Eq. 1: Fig. 2 shows the value of B_2 in both collision systems. For both cases the in-jet coalescence parameter is enhanced with respect to the

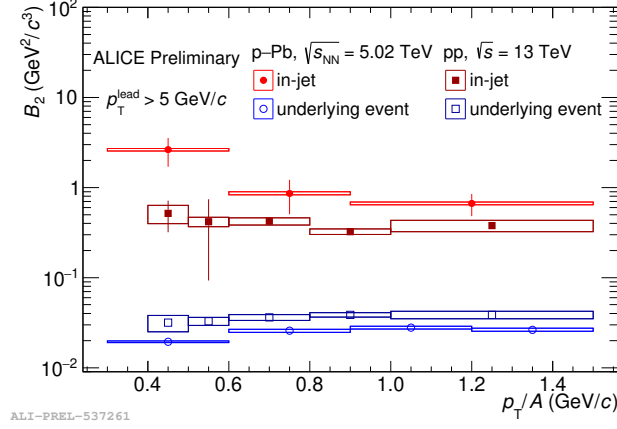


Figure 2: Coalescence parameter B_2 in jet (red) and in underlying event (blue) as a function of the transverse momentum divided by the mass number of the nucleus, for both pp collisions at $\sqrt{s} = 13$ TeV (darker points) [18] and p–Pb collisions at $\sqrt{s_{NN}} = 5.02$ TeV (brighter points). Vertical bars represent the statistical uncertainties while boxes represent the systematic uncertainties.

same quantity in the underlying event, with a factor of about 15 for the pp case and a factor about 24 for the p–Pb case. Focusing on the underlying event part, a smaller value of B_2 is observed in p–Pb collisions: this is predicted by the coalescence model, since the source size of the p–Pb system is slightly larger with respect of the pp system, 1.5 fm [20] against 1 fm [21]. Looking at the in-jet part, instead, the coalescence parameter is larger in p–Pb collisions with respect to pp ones: assuming the same source size for the nucleons in the jet, the nucleons are probably more close in momentum space in the p–Pb case with respect to the pp case. On the other end, also the particle composition of the jet could affect the coalescence probability: Fig. 3 shows the deuteron-over-proton ratio for both the collision systems. In both cases, the ratio in-jet is larger with respect to the same quantity

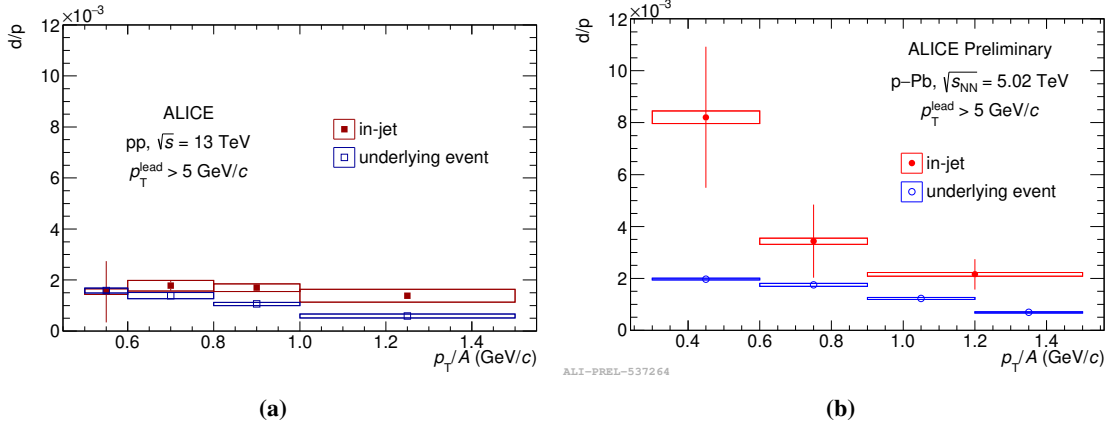


Figure 3: Deuteron-to-proton ratio in-jet (red) and in underlying event (blue) in pp collisions at $\sqrt{s} = 13$ TeV (left panel) [18] [22] and p–Pb collisions at $\sqrt{s_{NN}} = 5.02$ TeV. Vertical bars represent the statistical uncertainties while boxes represent the systematic uncertainties.

evaluated in the underlying event. Moreover, focusing on the in-jet case, the ratio is larger in p–Pb collisions, thus showing a different particle composition in the jet in the two collision systems.

However, the deuteron-to-proton ratio is affected by large uncertainties, and more data are needed to fully address this issue.

3. Comparison with models

The results from the pp collisions are compared to predictions of two different models. The first one, reported in the panel (a) of Fig 4, is based on PYTHIA 8 Monash 2013 tune [23] with a simple coalescence model, where the deuteron is formed if the momentum difference between proton and neutron is smaller with respect of a fixed value. In the second approach, showed in panel (b) of Fig. 4, the deuteron production is implemented with PYTHIA 8.3 [24] and described with ordinary reactions. In both cases the models gave a good qualitative description of the data, reproducing the large difference of about one order of magnitude between B_2^{jet} and B_2^{UE} . Moreover, the p_T/A dependence of B_2^{UE} is well described by both models within the uncertainties, while the B_2^{jet} trend is not well reproduced by the models, especially at low p_T/A .

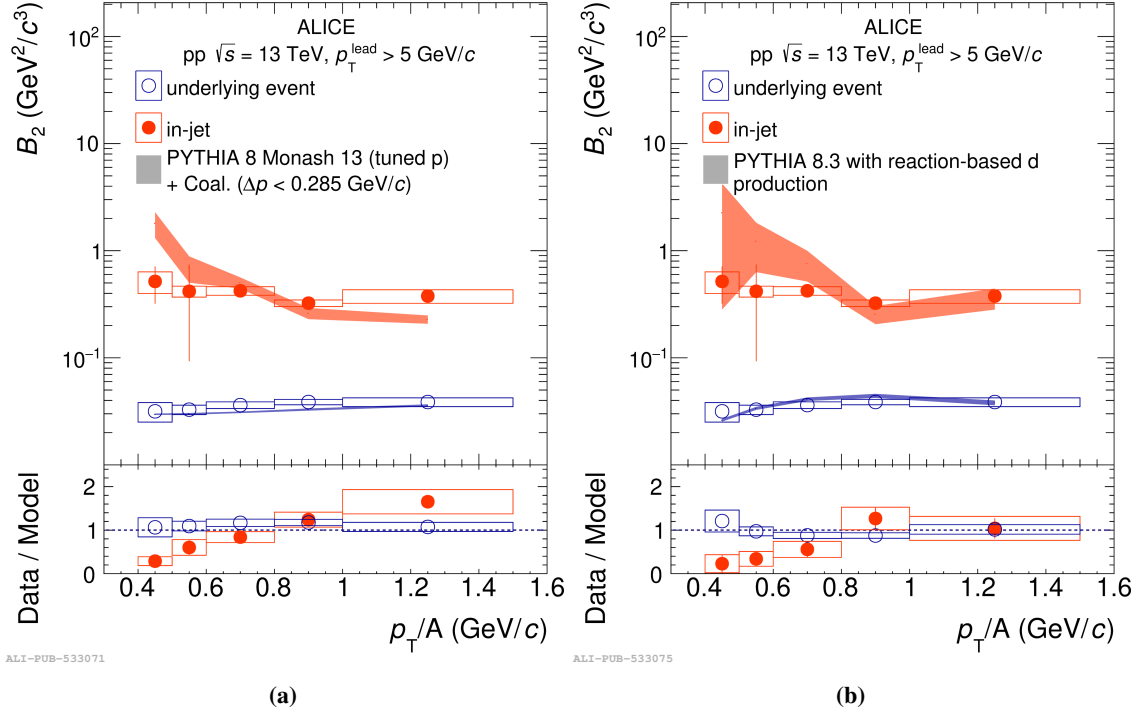


Figure 4: Coalescence parameter in jets and in the underlying event as a function of p_T/A , in comparison with the predictions from PYTHIA 8 Monash 2013 tune plus simple coalescence (panel (a)) and PYTHIA 8.3 with a reaction-based deuteron production (panel (b)). [18]. Vertical bars represent the statistical uncertainties while boxes represent the systematic uncertainties.

The measurement of the coalescence parameter in jet and underlying event will be improved thanks to the new data collected by ALICE during the Run3. The study will be performed considering a multi-differential approach, using jet finder algorithm to fully reconstruct the jet, and evaluating the dependence of the coalescence parameter from the jet radius.

References

- [1] E878 Collaboration, *Phys.Rev. C* **58** (1998) 1155-1164.
- [2] E864 Collaboration, *Phys. Rev. Lett.* **85** (2000) 2685–2688.
- [3] STAR Collaboration, *Phys. Rev. Lett.* **87** (2001) 2623011–2623016.
- [4] PHENIX Collaboration, *Phys. Rev. Lett.* **94** (2005) 122302.
- [5] BRAHMS Collaboration, *Phys. Rev. C* **83** (2011) 044906.
- [6] ALICE Collaboration, *Phys. Rev. C* **93** 2, (2016) 024917.
- [7] ALICE Collaboration, *Phys. Rev. C* **97** 2, (2018) 024615.
- [8] ALICE Collaboration, *Phys. Lett. B* **794** (2019) 50–63.
- [9] ALICE Collaboration, *Phys. Lett. B* **800** (2020) 135043.
- [10] ALICE Collaboration, *Eur. Phys. J.* **C80** 9, (2020) 889.
- [11] ALICE Collaboration, *Phys. Lett. B* **819** (2021) 136440.
- [12] ALICE Collaboration, *JHEP* **01** (2022) 106.
- [13] ALICE Collaboration, *Phys. Rev. Lett.* **128** 25 (2022) 252003.
- [14] A. Andronic, P. Braun-Munzinger, J. Stachel, H. Stöcker, *Phys. Lett. B* **697** (2011) 203-207.
- [15] S. T. Butler, C. A. Pearson, *Phys. Rev.* **129** (1963) 836.
- [16] A. Andronic, P. Braun-Munzinger, K. Redlich, J. Stachel, *Nature* **561** (2018) 321–330.
- [17] M. Mahlein et al, *Eur. Phys. J. C* **83** (2023) 804.
- [18] ALICE Collaboration, *Phys. Rev. Lett.* **131** (2023) 042301.
- [19] ALICE Collaboration, *JINST* **3** (2008) S08002.
- [20] ALICE Collaboration, *Phys. Rev. Lett.* **123**, (2019) 112002.
- [21] ALICE Collaboration, *Phys. Rev. C* **99**, (2019) 024001.
- [22] ALICE Collaboration, *JHEP* **06** (2023) 027.
- [23] P. Skands, S. Carrazza, J. Rojo, *Eur. Phys. J.* **C74**, (2014) 3024.
- [24] C. Bierlich et al, arXiv:2203.11601 [hep-ph].